

In Situ High-Energy Synchrotron Radiation Study of Sol–Gel Nanoparticle Formation in Supercritical Fluids**

Henrik Jensen, Martin Bremholm, Rudi P. Nielsen, Karsten D. Joensen, Jan S. Pedersen, Henrik Birkedal, Yu-Sheng Chen, Jon Almer, Erik G. Sogaard, Steen B. Iversen, and Bo B. Iversen*

Nanostructured materials have drawn much attention because of the dramatically different properties observed on going from bulk material to nanosized particles. Nanoparticles have properties that lie between the quantum effects of atoms and molecules and the bulk properties of materials. In the nanometer range (1–100 nm) the particle size affects structural characteristics (e.g., lattice symmetry, unit-cell dimension), electronic properties (e.g., band gap), and therefore also the physical (e.g., wetting, melting point) and chemical properties (e.g., catalytic effects) of a material. The applications of nanomaterials include lithium-based batteries, fuel cells,^[1,2] thin films, inorganic–organic hybrid materials,^[3] sensors, piezoelectric devices, and catalysts.^[4,5] In all production methods for nanomaterials, a key requirement is the ability to control nanoparticle size, shape, and crystallinity. Special attention has been devoted to metal oxides. These can adopt many different crystal structures and have metallic,

semiconducting, or insulating properties.^[5] Their chemical properties range from strong catalytic reactivity to chemical inertness and high-temperature stability, and the application of metal oxides is a multibillion-dollar industry.

Several wet-chemistry synthesis routes are capable of producing nanomaterials,^[6] but the sol–gel technique has become the standard method for fabricating metal oxides because of the possibility of obtaining high chemical homogeneity at low temperature and under mild chemical conditions.^[5,7] The downside is the relatively long process time and the need for posttreatment (e.g., calcination), which make the process less attractive for industry. The solution appears to be synthesis in supercritical fluids, which provides unique control of chemistry and nanocrystal properties.^[8–17] Use of supercritical fluids as solvents in sol–gel processes enhances the kinetics by more than an order of magnitude. Furthermore, supercritical fluids exhibit particularly attractive properties such as gaslike mass-transfer behavior, liquid-like densities, and changed dielectric properties. These properties can be fine-tuned by simple changes in pressure and temperature; for example, the solubility of a compound can be dramatically changed to cause very fast precipitation.

To manipulate the properties of nanomaterials and synthesize new materials with unprecedented properties, the main challenge is to understand the nucleation, crystallization, and growth processes.^[5] This requires development of analytical tools capable of following nanoparticle formation in real time. In situ measurements by dynamic light scattering (DLS) have been used to study particle growth and stabilization of primary particles by surfactants.^[18] In situ synchrotron powder diffraction has become a widely used tool for following solid-state reactions and crystallization processes.^[19–21] The crux of this technique is the high intensity of the synchrotron beam, which allows data collection on a sufficiently short timescale of seconds to minutes. However, in the case of sol–gel processes, it is desirable to obtain information on particle size and size distributions besides data on sample crystallinity and crystallite size. This complicates the characterization task, and a combination of techniques must be used. These must work when the chemical environment changes rapidly under conditions employed in industrial chemical processes.^[5] Simultaneous, real-time, in situ small-angle X-ray scattering (SAXS) and wide-angle X-ray scattering (WAXS) potentially meet this challenge.

Here we present the first real-time, in situ characterization of nanoparticle formation in supercritical fluids. The supercritical environment seriously complicates the characteriza-

[*] M. Bremholm, Prof. Dr. J. S. Pedersen, Dr. H. Birkedal, Prof. Dr. B. B. Iversen
Department of Chemistry and
Interdisciplinary NanoScience Center
Langelandsgade 140, 8000 Aarhus C (Denmark)
Fax: (+45) 8942-3969
E-mail: bo@chem.au.dk
Dr. H. Jensen, R. P. Nielsen, Dr. S. B. Iversen
SCF-Technologies a/s
Gammel Koege Landevej 22 H, 2500 Valby (Denmark)
Dr. K. D. Joensen
JJ X-Ray Systems ApS
Gl. Skovlundevej 54, 2740 Skovlunde (Denmark)
Dr. Y. Chen
BioCARS/CARS
The University of Chicago
Advanced Photon Source/ANL, Argonne, IL 60439 (USA)
Dr. J. Almer
Advanced Photon Source (APS)
Argonne National Laboratory, Argonne, IL 60439 (USA)
Prof. E. G. Sogaard
Aalborg University Esbjerg
Colloid and Interface Chemistry Group
Niels Bohrs Vej 8, 6700 Esbjerg (Denmark)

[**] Use of the Advanced Photon Source was supported by the US Department of Energy, Office of Science, Office of Basic Energy Sciences, under contract no. W-31-109-Eng-38. Dansync is gratefully acknowledged for support. H.B. is funded by the Danish Research Councils.



Supporting information for this article is available on the WWW under <http://www.angewandte.org> or from the author.

tion task. To withstand the high pressures, thick reactor windows are crucial, but these absorb the probing X-rays unless the energy is very high. For high-energy X-rays ($E > 80$ keV) transmission becomes acceptable even for one-inch-thick borosilicate windows (70 % transmission). However, the incoming X-ray intensity must still be sufficiently high to give a time resolution of minutes. The experiments were conducted at Beamline 1-ID at APS at Argonne National Laboratory, one of the few synchrotron beamlines in the world where a sufficient flux of high-energy X-rays is available.^[22] The study used supercritical, seed-enhanced crystallization of anatase TiO_2 nanoparticles.^[23] TiO_2 is a preferred system for experimentalists because it is well suited for many experimental techniques.^[24] The combined real-time use of SAXS and WAXS provides fundamental insight into the mechanism of supercritical nanoparticle formation: nanoparticle formation follows the same progression seen in traditional solvothermal synthesis but on a much shorter timescale and at lower temperatures. This demonstrates how the use of supercritical media can bring nanomaterials production into a new timescale, and widespread applications can be expected.

Nanoparticle formation is shown in Figure 1, where the WAXS (b) and SAXS (c) curves are plotted as a function of time. In the first 20 min of the experiment, the SAXS curves are those of a “wet gel”.^[24,25] After the gelation period a transformation period is observed from 20 to 80 min, which is followed by slow particle growth. The final SAXS curves are similar to earlier ex situ SAXS measurements for this process,^[26] which are characterized by a broad peak around a scattering vector of $q = 0.028 \text{ \AA}^{-1}$ that reflects the mean

particle diameter. The size distributions were extracted by the hard-sphere model^[27–29] after the gelation period ($t > 20$ min). The size of the primary particles changes during the transition stage and stabilizes after 50 min at a volume-weighted diameter of 6.8 nm. The time dependence of the anatase (200) reflection (Figure 1b) clearly shows development of crystalline particles.

To investigate the mechanism of nanoparticle formation, the intensity at $q = 0.028 \text{ \AA}^{-1}$ for the SAXS curves was compared to the integrated intensity of the anatase (200) peak, which is shown in the Figure 2a. In Figure 2b, the extracted crystallite sizes obtained from the Scherrer formula^[30] and the volume-weighted primary particle sizes (diameters) extracted from the SAXS curves are plotted. The anatase (200) and the $q = 0.028 \text{ \AA}^{-1}$ SAXS intensity show exactly the same time dependence, that is, the particle growth seen in SAXS parallels the development of crystallinity. The supercritical formation of nanoparticles is characterized by four distinct periods: an induction period (A), a latent period (B), a precipitation period (C), and a slow growth period (D). This behavior corresponds to that known in conventional sol-gel syntheses.^[31] However, the supercritical medium leads to much faster reactions compared to conventional sol-gel chemistry.^[32,33]

A series of experiments was performed in which heating rate, final reaction temperature, and precursor concentration were varied. Here we compare four experiments, which are summarized in Table 1. The crystallization temperature T_A was found to be $(87 \pm 5)^\circ\text{C}$ for all experiments, while the latent period t_A is influenced by both precursor concentration and heating rate. The precipitation period is longer for

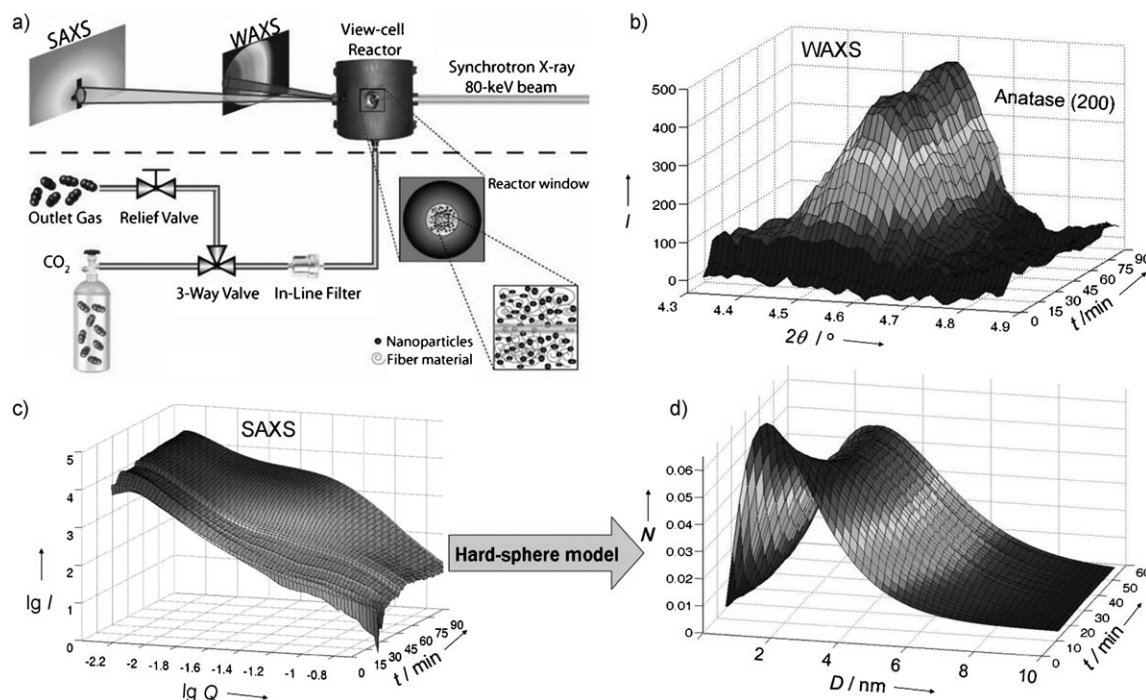


Figure 1. Experimental setup for real-time, in situ SAXS/WAXS studies of supercritical reactions (a). The development of crystallinity can be monitored by WAXS, as exemplified by the anatase (200) reflection (b). The SAXS data (c) provide information on mesostructure, and particle size distribution (diameter) was extracted by using a hard-sphere model (d).

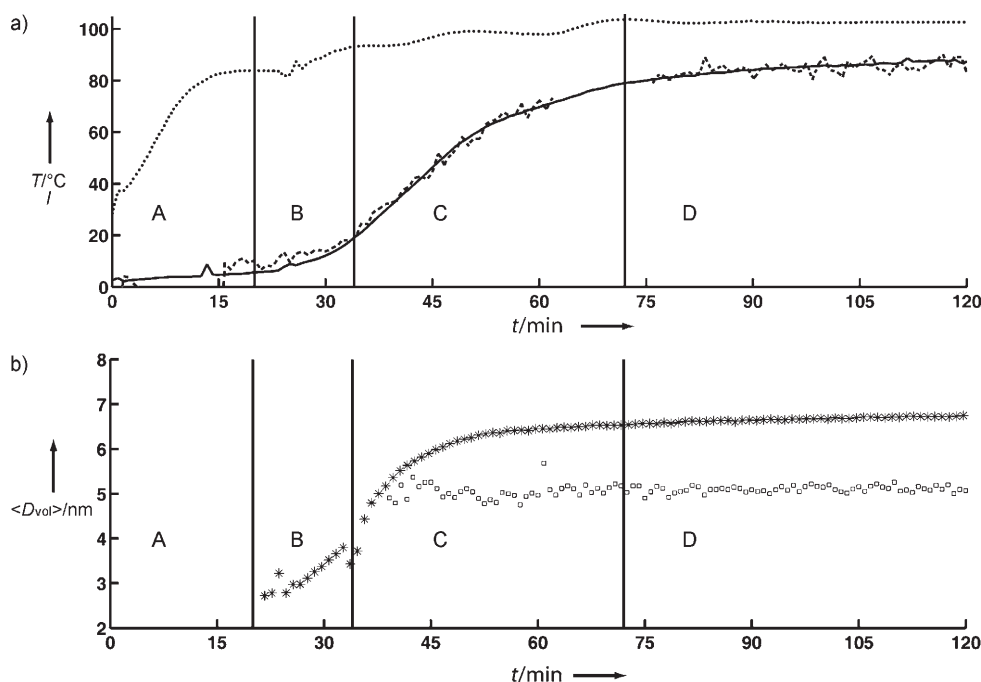


Figure 2. Particle formation: a) SAXS intensity (—), WAXS anatase (200) area (---), and temperature (.....) as a function of time. b) Volume-weighted sizes D_{vol} determined from SAXS (★) and WAXS (□).

Experiment 2 because of the low heating rate but very short for Experiment 4. This is also seen in the growth rate for the precipitation period r_C , which for Experiment 4 is increased by a factor of four compared to the three other experiments.

Table 1 also lists the in situ extracted particle (d_p) and crystallite sizes ($D_{in situ}$). The primary particle sizes are around

Table 1: Comparison of extracted particle properties.

Experiment	1	2	3	4
T_{final} [°C] ^[a]	100	100	100	125
T_{grad} [%] ^[b]	100	33	100	100
V_{TTIP} [mL] ^[c]	2.1	2.1	6.1	6.3
t_A [min] ^[d]	20	45	8	8
T_A [°C] ^[e]	84	86	92	82
t_B [min] ^[f]	14	68	3	4
t_C [min] ^[g]	38	55	44	13
r_C [min ⁻¹] ^[h]	0.021	0.013	0.019	0.058
d_p [nm] ^[i]	6.8	6.9	6.3–6.8	7.2
$D_{in situ}$ [nm] ^[j]	5.1	5.1	4.0–5.1	4.0–5.1

[a] Final reaction temperature. [b] Measure of the heating rate. [c] Volume of the titanium precursor. [d] Induction period. [e] Crystallization temperature. [f] Latent period. [g] Precipitation period. [h] Growth rate during precipitation. [i] Average primary particle size. [j] Crystallite size for Period D (slow growth period).

30–40% larger than the crystallite sizes. The discrepancy between primary particle size and crystallite size is likely caused by the presence of an amorphous fraction, which contributes to the SAXS size, but not to the size determined by WAXS. Transmission electron micrographs show that the particles are spherical, which proves that the difference

between the size estimates does not result from anisotropic particle shape (see Supporting Information).

The results presented here demonstrate that nanoparticle formation in supercritical media can be followed in situ by simultaneous SAXS/WAXS with high-energy synchrotron radiation. The technique provides a direct means for optimizing process parameters in specific applications. The supercritical sol-gel process parallels the characteristics of conventional sol-gel processes but at unprecedented low temperatures and in a new timescale. In supercritical fluids sol-gel processes occur in minutes rather than hours. This greatly improves the efficient fabrication of high-quality nanomaterials.

Experimental Section

A supercritical seed-enhanced crystallization (SSEC) process was studied during the formation of nanocrystalline TiO_2 . The SSEC process involves a sol-gel reaction in supercritical CO_2 that takes place in the proximity of a seeding material.^[23] The in situ setup (Figure 1a) is centered on a custom-made stainless steel viewing-cell reactor (30 mL) with two 12.7-mm (0.5-inch) borosilicate windows, which is placed in the synchrotron beam. In a typical experiment, the reactor was loaded with seed material, titanium precursor (titanium tetraisopropoxide, TTIP), and deionized water. The hydrolysis ratio ($HR = [H_2O]/[TTIP]$) was kept constant at 7.87 for all experiments, and polypropylene fiber (PP) was chosen as seeding material. The reactants were separated by the PP and mixing occurred instantaneously when CO_2 was added to the system. The reactor was pressurized to 100 bar with CO_2 and the temperature was raised to 373 K. The WAXS and SAXS CCD detectors (time resolution 50 s) were placed 1.3 m and 5 m from the reactor cell, respectively, providing an accessible diffraction angle of 1.5 – 7.5° (2θ) and a SAXS q range of 0.005 – 0.25 \AA^{-1} .

Received: August 18, 2006

Revised: November 3, 2006

Published online: January 4, 2007

Keywords: crystal growth · nanostructures · sol-gel processes · supercritical fluids · X-ray scattering

- [1] A. S. Aricò, P. Bruce, B. Scrosati, J. Tarascon, W. van Schalkwijk, *Nat. Mater.* **2005**, *4*, 366–377.
- [2] K. Kang, Y. S. Meng, J. Breger, C. P. Grey, G. Ceder, *Science* **2006**, *311*, 977–980.
- [3] C. Sanchez, G. J. D. A. A. Soler-Illia, F. Ribot, D. Grosso, C. R. Chim. **2003**, *6*, 1131–1151.

- [4] C. Burda, X. Chen, R. Narayanan, M. A. El-Shayed, *Chem. Rev.* **2005**, *105*, 1025–1102.
- [5] M. Fernández-García, A. Martínez-Arias, J. C. Hanson, J. A. Rodríguez, *Chem. Rev.* **2004**, *104*, 4063–4104.
- [6] B. L. Cushing, V. L. Kolesnichenko, C. J. O'Connor, *Chem. Rev.* **2004**, *104*, 3893–3946.
- [7] C. J. Brinker, G. W. Scherer, *Sol–Gel Science: The Physics and Chemistry of Sol–Gel Processing*, Academic Press, London, **1990**.
- [8] F. Cansell, B. Chevalier, A. Demourgues, J. Etourneau, C. Even, Y. Garrabos, V. Pessey, S. Petit, A. Tressaud, F. Weill, *J. Mater. Chem.* **1999**, *9*, 67–75.
- [9] J. D. Holmes, D. M. Lyons, K. J. Ziegler, *Chem. Eur. J.* **2003**, *9*, 2144–2150.
- [10] K. P. Johnston, P. S. Shah, *Science* **2004**, *303*, 482–483.
- [11] J. Jung, M. Perrut, *J. Supercrit. Fluids* **2001**, *20*, 179–219.
- [12] P. S. Shah, T. Hanrath, K. P. Johnston, B. A. Korgel, *J. Phys. Chem. B* **2004**, *108*, 9574.
- [13] E. Reverchon, R. Adami, *J. Supercrit. Fluids* **2006**, *37*, 1–22.
- [14] J. A. Darr, M. Poliakoff, *Chem. Rev.* **1999**, *99*, 495–541.
- [15] F. Cansell, C. Aymonier, A. Loppinet-Serani, *Curr. Opin. Solid State Mater. Sci.* **2003**, *7*, 331–340.
- [16] P. G. Smith, W. Ryoo, K. P. Johnston, *J. Phys. Chem. B* **2005**, *109*, 20155–20165.
- [17] T. Adschiri, K. Kanazawa, K. Arai, *J. Am. Ceram. Soc.* **1992**, *75*, 1019–1022.
- [18] K. T. Lim, H. S. Hwang, S.-S. Hong, W. Ryoo, K. P. Johnston, *Langmuir* **2004**, *20*, 2466–2471.
- [19] A. K. Cheetham, C. F. Mellot, *Chem. Mater.* **1997**, *9*, 2269–2279.
- [20] R. J. Davey, W. Liu, M. J. Quayle, J. T. Tiddy, *Cryst. Growth Des.* **2002**, *2*, 269–272.
- [21] N. Lyakhov, Y. Gaponov, B. Tolochko, *Solid State Ionics* **1997**, *101*, 1251–1256.
- [22] H. Jensen, *Supercritical Production of Nanoparticles*, Ph.D. Thesis, Aalborg University Esbjerg, **2006**, ISBN 87-7606-013-6.
- [23] H. Jensen, K. D. Joensen, S. B. Iversen, E. G. Sogaard, *Ind. Eng. Chem. Res.* **2006**, *45*, 3348–3353.
- [24] J. M. Barthez, F. Molino, J. Marignan, A. Ayrat, C. Guizar, R. Jullien, *J. Sol-Gel Sci. Technol.* **1997**, *8*, 83–88.
- [25] V. Torma, H. Peterlik, U. Bauer, W. Rupp, N. Husing, S. Bernstorff, M. Steinhart, G. Goerigk, U. Schubert, *Chem. Mater.* **2005**, *17*, 3146–3153.
- [26] H. Jensen, J. H. Pedersen, J. E. Jørgensen, J. S. Pedersen, K. D. Joensen, S. B. Iversen, E. G. Sogaard, *J. Exp. Nanoscience* **2006**, *1*, 355–373.
- [27] J. S. Pedersen, *Phys. Rev. B* **1993**, *47*, 657–665.
- [28] J. S. Pedersen, *Adv. Colloid Interface Sci.* **1997**, *70*, 171–210.
- [29] J. S. Pedersen in *X-Rays and Light* (Eds.: P. Lidner, T. Zemb), Elsevier, Amsterdam, **2002**, chap. 16.
- [30] A. Guinier, *X-Ray Diffraction—In Crystals, Imperfect Crystals, and Amorphous bodies*, Dover Publication, New York, **1963**.
- [31] J. W. Mullin, *Crystallization*, 4th ed., Elsevier Butterworth-Heinemann, **2004**.
- [32] H. I. Hsiang, S. C. Lin, *Mater. Chem. Phys.* **2006**, *95*, 275.
- [33] H. Zhang, J. F. Banfield, *Chem. Mater.* **2002**, *14*, 4145.